analytical chemistry

Article

pubs.acs.org/ac

Versatile Electrochemiluminescent Biosensor for Protein–Nucleic Acid Interaction Based on the Unique Quenching Effect of Deoxyguanosine-5′-phosphate on Electrochemiluminescence of CdTe/ZnS Quantum Dots

Peng Zhao, Lifen Zhou, Zhou Nie,* Xiahong Xu, Wang Li, Yan Huang, Kaiyu He, and Shouzhuo Yao

State Key Laboratory of Chemo/Biosensing and Chemometrics, College of Chemistry and Chemical Engineering, Hunan University, Changsha, 410082, People's Republic of China

Supporting Information

ABSTRACT: In this paper, the efficient quenching effect of deoxyguanosine-5′-phosphate (dGMP) on anodic electrochemiluminescence (ECL) of the CdTe/ZnS quantum dots (QDs) is reported for the first time. This ECL quenching was found to be specific for free dGMP and not observed for dGMP residues in different DNA structures. The unique dGMP-based QDs ECL quenching was then utilized to develop a versatile biosensing strategy to determine various protein–DNA interactions with the assistance of exonuclease, Exo I, to hydrolyze DNA and liberate dGMP. Taking single-stranded DNA binding protein (SSB) and thrombin as examples, two novel detection modes have been developed based on dGMP–QDs ECL strategy. The first method used hairpin probes and SSB-promoted probe cleavage by Exo I for facile signal-off detection of SSB, with a wide linear range of 1–200 nM and a low detection limit of 0.1 nM. The second method exploited aptamer–thrombin binding to protect probes against Exo I degradation for sensitive signal-on detection of thrombin, giving a linear response over a range of 1–150 nM and a detection limit as low as 0.1 nM. Both methods were homogeneous and label-free without QDs or DNA modification. Therefore, this dGMP-specific QDs ECL quenching presents a promising detection mechanism suitable for probing various protein–nucleic acid interactions.

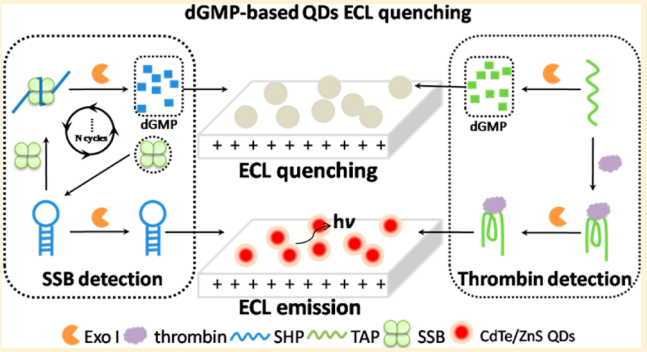

Quantum dots (QDs) including a number of nanoparticles composed by IIA–VIA semiconductors or IIIA–VA semiconductors have attracted great interest.[1−5] Because of their outstanding luminescent properties of size-tunable emission wavelength, superior brightness, and remarkable photostability, they have been widely exploited in barcoding labeling,[6,7] biosensing, and medical imaging.[8−12] Compared with the well-developed fluorescent applications of QDs, the electrochemiluminescence (ECL) of QDs is an emerging application bearing intrinsic features including low cost, absence of a background optical signal, and high sensitivity, which was first reported by Bard's group in organic media.[13] As a newcomer in ECL materials family, the QDs-ECL possesses many advantages over traditional ECL emitters, such as controllable electrochemical and ECL properties defined by quantum size effect. Due to these intriguing merits, constant efforts have been devoted to systematically investigate the ECL phenomenon of QDs and relevant mechanism. Two dominant pathways for ECL generation of QDs, annihilation and coreactant pathways, have been successively demonstrated.[14] In the annihilation process, the oxidized and reduced forms of QDs can be electrochemically produced by sweeping both positive and negative voltages and these two species react with each other to form an excited state and correspondingly emit ECL. With the assistance of coreactants, the ECL phenomenon of QDs also can be observed by potential sweeping at only positive or negative voltages, namely, anodic or cathodic ECL of QDs. Two kinds of coreactants were involved: one group would facilitate the production of redox species of QDs which are a necessary counterpart in annihilation of QDs but cannot be directly electrogenerated on the surface of electrode, such as O_2 in anodic ECL and H_2O_2 in cathodic ECL;[15] the other group normally presents in cathodic ECL of QDs, and its intermediate directly interacts with electrogenerated reduced QDs via electron transfer to yield excited species, for instance, $S_2O_8^{2-}$.[16−18]

The increasing understanding of the ECL mechanism of QDs promotes the development of new biosensing strategies based on QDs ECL. The pioneering works focused on the straightforward detection of coreactants and their relative

Received: February 9, 2013
Accepted: June 6, 2013

   dx.doi.org/10.1021/ac4004437 | Anal. Chem. XXXX, XXX, XXX–XXX

generator or quencher. The first QDs ECL sensor that used cathodic ECL of CdSe QDs for H_2O_2 detection was fabricated by Ju's group.[15] On the basis of this, they further developed a series of QDs ECL biosensors for detection of glucose by enzymatic generation of H_2O_2,[19] immunoassay via H_2O_2 diminishing by labeled-horseradish peroxidase,[20] and measurement of thiols through quenching the hydroxyl radical,[21] an important intermediate in cathodic ECL of QDs. Moreover, they successfully achieved the anodic ECL of CdTe QDs for ECL detection of catechol via energy transfer between excited QDs and the oxidation product of catechol.[22] An ECL immunoassay for detection of low-density lipoproteins (LDLs) based on cathodic ECL of CdS QDs has been developed on the basis of inhibition effect of LDL binding on accessibility of coreactant $S_2O_8^{2-}$ to the electrode.[16] Another interesting example is the low-potential ECL sensing of Cu^{2+} and Hg^{2+} dependent on surface unpassivation of CdTe QDs and competition of analyte cation to stabilizer.[8] Recently, the unique properties of the composite of QDs and other nanomaterials have attracted increasing attentions and provide the potential to fabricate new QD ECL biosensing platform. Carbon nanotubes and graphene oxides have been discovered to amplify the ECL intensity of CdTe QDs, exhibiting high sensitivity to H_2O_2 and good selectivity in glutathione sensing.[23,24] Two distinct effects of gold nanoparticles (AuNPs) on ECL of QDs, plasmonic resonance-induced enhancing and energy transfer-caused quenching, were both demonstrated and implemented in the detection of thrombin by aptamer recognition and single-nucleotide polymorphism via isothermal amplification.[9,25] To date, although multifarious sensing mechanisms of QDs ECL have been developed, most of them are related to ion or small-molecule detection. Notably, at present, only two mechanisms based on AuNPs−QDs interaction and direct usage of QDs as ECL labels[26,27] are available for DNA-related biosensing, especially protein−DNA interaction assays, which are crucial in biological research. Furthermore, all these methods required the chemical modification of QDs and AuNPs for DNA labeling, remarkably increasing the cost and complexity of the assays. Hence, the development of novel QDs ECL approaches suitable for the label-free detection of protein−DNA interaction is still highly in demand.

Protein−DNA interactions play a pivotal role in a wide variety of important biological processes involved in DNA metabolism, such as DNA replication, transcription, recombination, and repair. In the present work, we have proposed a novel label-free ECL sensing platform versatile for detection of various protein−DNA interactions based on unique quenching effect of deoxyguanosine-5′-phosphate (dGMP) on ECL of CdTe/ZnS QDs and enzymatic DNA cleavage by exonuclease. We are curious about the influence of nucleotides, the essential ingredient of DNA, on QDs ECL, which is important but still unexplored to date. We have systematically investigated four deoxynucleotides in the QDs ECL experiments and found that only deoxyguanosine-5′-phosphate (dGMP) could significantly quench the ECL intensity of CdTe/ZnS QDs. This intriguing phenomenon has been extended to DNA-related biosensing by exploiting the digestion function of the exonuclease I (Exo I), which catalyzes the removal of nucleotides from single-stranded DNA in the 3′ to 5′ direction. To prove the feasibility of the proposed method, two typical DNA−protein interactions, the binding of single-stranded DNA (ssDNA) by ssDNA binding protein (SSB) and the recognition of thrombin by its specific aptamer, were chosen as the models in this study. Two distinct sensing approaches have been established based on the intrinsic properties of the relative protein−DNA interactions: a signal-off design for SSB relied on the ssDNA−SSB binding-stimulated exonuclease digestion and a signal-on design for thrombin by aptameric binding protection against exonuclease digestion. All these designs are label-free, and both QDs and DNA are unmodified. Therefore, this dGMP-based QDs ECL quenching presents not only a new detection mechanism for QDs ECL analytical applications but also a promising way to study various protein−DNA interactions.

EXPERIMENTAL SECTION

Materials. Oligonucleotides used in this study were synthesized by Sangon (Shanghai, China) and confirmed by mass spectrometry. Table 1 shows the sequences of the used oligonucleotides. SSB was purchased from Promega (Madison, WI, U.S.A.). KCl, Tris(hydroxymethyl)aminomethane (Tris), deoxyadenosine-5′-phosphate (dAMP), dGMP, deoxycytidine-5′-phosphate (dCMP), deoxythymidine-5′-phosphate (dTMP), and thrombin were purchased from Sigma-Aldrich (St. Louis, MO, U.S.A.). Exo I and 10× Exo I buffer (670 mM glycine−KOH, 67 mM $MgCl_2$, 10 mM DTT, pH 9.5) were purchased from the Fermentas (Vilnius, Lithuania). CdTe/ZnS QDs with thioglycolic acid (TGA) as ligand were purchased from ZhongDS (Shenzhen, China). Ultrapure water obtained from a Millipore Milli-Q system (18.2 MΩ·cm) was used in all runs. Other chemicals were all of analytical grade.

Table 1. Sequences of the Used Oligonucleotides (in the 5′ to 3′ Direction)[a]

type	sequence
P1	5′-CCC TAA CCC TAA CCC TAA CCC TAA ATG CA-3′
P2	5′-TGC ATT TAG GGT TAG GGT TAG GGT TAG GG-3′
SHP-1	5′-**GCT CG**G TGA TAG GGA AGA AGG AAG **CGA GC**-3′
SHP-2	5′-**GAC TCG** GTG ATA GGG AAG AAG GAA G**CG AGT C**-3′
SHP-3	5′-**GAC TCT G**GT GAT AGG GAA GAA GGA AG**C AGA GTC**-3′
TAP-1	5′-***GGT TGG TGT GGT TGG***-3′
TAP-2	5′-GGT TGG T***GG TTG GTG TGG TTG G***-3′
TAP-3	5′-GGT TGG TGG TTG GT***G GTT GGT GTG GTT GG***-3′
random	5′-AGA AGA ACC TGT CTC AGT A-3′

[a]The underlined bold letters of SHP-1, SHP-2, and SHP-3 are the stem complementary sequence of the hairpin. The italic bold letters of TAP-1, TAP-2, and TAP-3 are the sequence of thrombin aptamer.

Apparatus. Fluorescence spectra were recorded using a 1 cm path length quartz cuvette on a Hitachi F-4500 spectrometer. The electrochemical and ECL measurements were carried out on an MPI-A multifunctional electrochemical and chemiluminescent analytical system (Remex, Xi'an, China) at room temperature with a configuration consisting of an indium/tin oxide (ITO) working electrode, a platinum counter electrode, and a Ag/AgCl (saturated KCl solution) reference electrode. The emission window was placed in front of the photomultiplier tube set at −800 V. The ITO electrodes with a working area of 0.5 cm^2 were purchased from Laibao (Shenzhen, China). The ECL spectrum was measured by collecting the ECL data at +1.38 V during cyclic potential sweep with nine pieces of long-pass filters at cutoff wavelengths of 500, 520, 550, 580, 600, 630, 650, 670, and 700 nm, and the

dx.doi.org/10.1021/ac4004437 | Anal. Chem. XXXX, XXX, XXX−XXX

data were fitted in accordance with reported literature. Their thickness was 2 mm, and transparent efficiency was 88%.

ECL Detection of SSB Based on SSB-Stimulated Exo I Cleavage. The SSB detection was performed in binding buffer (20 μL, 67 mM glycine−KOH, 6.7 mM $MgCl_2$, pH 9.5).The SSB hairpin probe (SHP-1, SHP-2, or SHP-3, 0.25 μM) was prepared by heating to 90 °C for 4 min, then cooling to room temperature over approximately 5 min to form a beacon structure. For SSB detection, different concentration of SSB was added to SHP solution and the mixture was incubated for 10 min. Then 2 U/μL Exo I was added, and the mixture was incubated for 30 min at 37 °C. ECL was recorded after 5 μL of resulting SSB detection solution was added to the 200 μL of 0.05 mg/mL CdTe/ZnS QDs solution in 0.01 M Tris−HCl buffer (pH 9.0), and the linear scan potential (0−1.5 V) was applied with a scan rate of 100 mV/s. Within each experiment the values were measured three times.

ECL Detection of Thrombin Based on Exo I Protection Assay. The thrombin aptamer probe (TAP-1, TAP-2, or TAP-3, 0.25 μM) in binding buffer (40 μL, 67 mM glycine−KOH, 6.7 mM $MgCl_2$, pH 9.5) was incubated with different concentration of thrombin at room temperature for 1 h to allow complete binding. Then, 2 U/μL of Exo I was added to the mixture and incubated at 37 °C for 0.5 h, followed by a heating step at 80 °C for 15 min to inactivate the Exo I. After this step, ECL was recorded after the resulting thrombin detection solution (5 μL) was added to the 0.05 mg/mL CdTe/ZnS QDs solution in 0.01 M Tris−HCl buffer (pH 9.0), and the linear scan potential (0−1.5 V) was applied with a scan rate of 100 mV/s. Within each experiment the values were measured three times.

Please see the Supporting Information for the experimental details of the preparation of 8-oxo-7,8-dihydro-2′-deoxyguanosine 5′-monophosphate (8-oxo-dGMP) and SSB activity assays by gel electrophoresis.

RESULTS AND DISCUSSION

Characterization of CdTe/ZnS QDs ECL. As illustrated in Supporting Information Figure S1, the peak of the CdTe/ZnS QDs ECL emission on the ITO electrode was located at +1.38 V, with an onset potential of +0.75 V. This peak potential of ECL emission was higher than that was needed for the ECL of CdTe QDs on the ITO electrode (+1.17 V),[22] probably owing to the surface passivation of the core/shell structure. Similar emission peaks at 610 and 600 nm were observed in the anodic ECL and fluorescence (FL, excited at 350 nm) spectra of CdTe/ZnS QDs, respectively (inset of Supporting Information Figure S1), indicating that the ECL emission, identical to the FL process, resulted from the transition of the excited state of CdTe/ZnS QDs*, was in consistency with prior research about CdTe QDs.[22,28] To evaluate whether the mechanism of CdTe/ZnS QDs anodic ECL is coreactant-involved, we investigated the effects of $O_2^{\bullet-}$ on this system. Both the addition of superoxide dismutase (SOD) as a $O_2^{\bullet-}$ scavenger (Supporting Information Figure S2A) and the usage of nitrogen-saturated solution to eliminate dissolved O_2 (Supporting Information Figure S2B) can significantly diminish ECL intensity of CdTe/ZnS QDs, demonstrating that the $O_2^{\bullet-}$ from the reduction of dissolved oxygen facilitates the ECL of CdTe/ZnS QDs. Therefore, the whole process of anodic ECL emission of CdTe/ZnS QDs is similar to that of its core-only counterpart CdTe QDs,[22] as described in the following equations:

$$\text{CdTe/ZnS QDs} + \text{In/SnO}_x \rightarrow \text{CdTe/ZnS QDs}\,(h^+) + \text{In/SnO}_x\,(e^-) \quad (1)$$

$$O_2 + \text{In/SnO}_x\,(e^-) \rightarrow O_2^{\bullet-} + \text{In/SnO}_x \quad (2)$$

$$\text{CdTe/ZnS QDs} + O_2^{\bullet-} \rightarrow \text{CdTe/ZnS QDs}\,(e^-) + O_2 \quad (3)$$

$$\text{CdTe/ZnS QDs}\,(h^+) + \text{CdTe/ZnS QDs}\,(e^-) \rightarrow \text{CdTe/ZnS QDs}^* \quad (4)$$

$$\text{CdTe/ZnS QDs}^* \rightarrow \text{CdTe/ZnS QDs} + h\upsilon \quad (5)$$

Quenching ECL of CdTe/ZnS QDs by dGMP. As shown in Figure 1A, the anodic ECL intensity of CdTe/ZnS QDs at

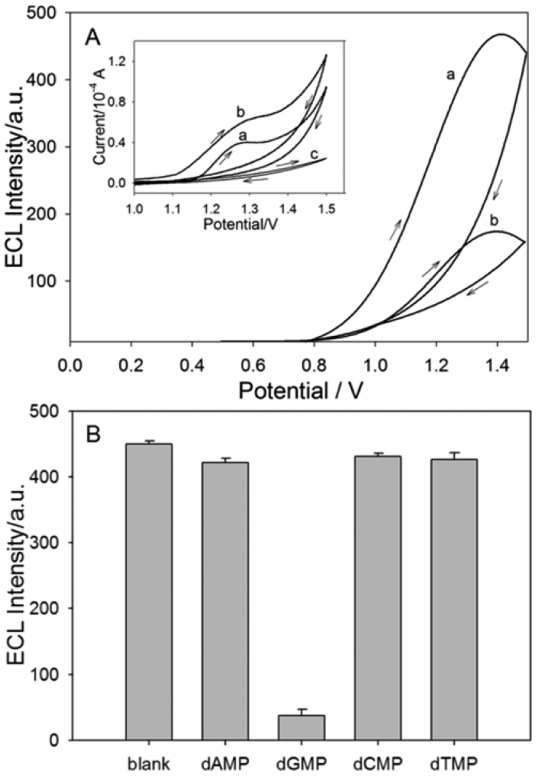

Figure 1. (A) Cyclic ECL and voltammetric curves (inset) of 0.05 mg/mL CdTe/ZnS QDs in air-saturated Tris−HCl buffer (pH = 9.0) at ITO electrodes before (a) and after (b) addition of 2.5 μM dGMP. Scan rate: 100 mV/s. Cyclic voltammetric curve c in the inset is the sample with only 2.5 μM dGMP. (B) The ECL intensity of CdTe/ZnS QDs measured at +1.38 V in the presence of 20 μM different deoxynucleotides.

+1.38 V was quenched 63% after addition of 2.5 μM dGMP, while the corresponding cyclic voltammograms (inset of Figure 1A), interestingly, showed that the electrooxidative current of QDs at peak potential of 1.25 V increased from 35 μA (Figure 1A, curve a) to 52 μA (Figure 1A, curve b) in the presence of dGMP. However, 2.5 μM dGMP only shows no detectable oxidation peak (Figure 1A, curve c) because ITO electrode is a kinetically poor oxidant for nucleobases.[29] The effects of deoxynucleotides on ECL of the CdTe/ZnS QDs (0.05 mg/mL CdTe/ZnS QDs) were further investigated by introducing 20 μM of four kinds of deoxynucleotides, dAMP, dGMP, dCMP, and dTMP. It was found that only dGMP could

dx.doi.org/10.1021/ac4004437 | Anal. Chem. XXXX, XXX, XXX−XXX

produce up to 92% quenching of ECL intensity (Figure 1B) and the others exhibited negligible effects, implying the deoxynucleotide-induced QD ECL quenching is selective and specific for dGMP.

It was discovered that the ECL efficiency of QDs was highly susceptible to solution pH value; thus, we carefully investigated the effect of pH on QDs ECL in the absence and presence of dGMP, respectively. As depicted in Supporting Information Figure S3, in spite of the presence of dGMP, the pH-dependent ECL intensity change exhibited the same trend. It showed a gradual increase with increasing pH from 7.5 to 9.0 and then turned to a rapid decrease. This optimal pH for QDs ECL at 9.0 was the same as reported in the literature.[22] Furthermore, the ECL quenching caused by dGMP under different pH values is illustrated in the inset of Supporting Information Figure S3, which also implies that the quenching efficiency at pH = 9.0 was the highest. Hence, the pH = 9.0 was chosen for the following ECL experiments.

The further quantitative measurement (Figure 2) showed a quick decrease of ECL intensity occurred in the range of 0−5 μM dGMP and tended to complete quenching at 20 μM dGMP with 0.05 mg/mL CdTe/ZnS QDs. This dGMP concentration dependence of QDs ECL quenching could be described by a Stern−Volmer equation: $I_0/I = 1 + K_{sv}[Q]$, where I_0 is the initial ECL intensity, I is the ECL intensity at a given concentration of quencher $[Q]$, and K_{sv} is the quenching constant. K_{sv} was found to be 4.9×10^5 M^{-1}. This relatively large value of K_{sv} allows this QD−ECL-based method to sensitively detect dGMP with a wide linear range from 50 nM to 2.5 μM and a detection limit of 30 nM. The relative standard deviation for three measurements at the dGMP concentration of 2.5 μM was 4.7%, indicating an acceptable reproducibility.

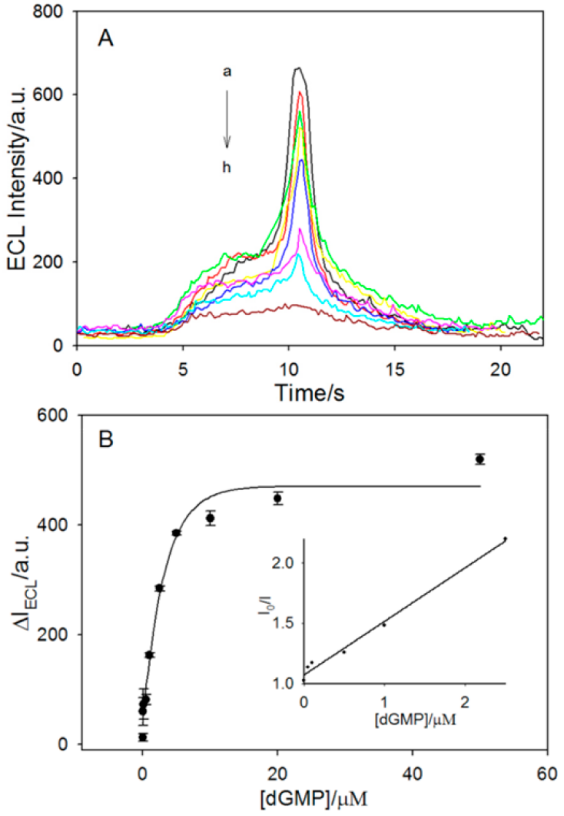

Figure 2. (A) ECL intensity−time behaviors of CdTe/ZnS QDs before (a) and after addition of 0.05, 0.1, 0.5, 2.5, 5, 10, and 50 μM (from b to h) dGMP in pH 9.0 Tris−HCl buffer. (B) Relationship between ECL quenching and dGMP concentrations ranging from 0.05 to 50 μM. Inset: linear calibration plot for dGMP.

Next, quenching mechanism of QDs by dGMP was explored. First, the effect of dGMP on the excited state of QDs (QDs*) was observed. As shown in Supporting Information Figure S4, increasing concentration of dGMP from 2.5 to 50 μM not only shows no quenching effect but a slight enhancement of the fluorescence of CdTe/ZnS QDs, proving that the quenching of ECL was not due to the quenching of the excited state. Second, the interaction of dGMP with intermediates of ECL was another possible quenching route. Although no direct oxidation of 2.5 μM dGMP was detectable on an ITO electrode, significant enhancement of QDs oxidation peak was observed in the presence of 2.5 μM dGMP. Similar phenomena were reported for $Ru(bpy)_3^{2+}$ electrochemical oxidation, and the $Ru(bpy)_3^{2+}$ electrochemical catalytic oxidation of guanine has been widely investigated.[30−33] Accordingly, we speculated that the remarkable increase of oxidation peak in QD/dGMP mixture is probably resulted from that the oxidized form of QD (QD^+) could oxidize guanine bases in an electrochemical catalytic pathway as follows:

$$QDs \rightarrow QDs^+ + e^- \quad \text{(at electrode)} \tag{6}$$

$$QDs^+ + \text{guanine} \rightarrow QDs + \text{guanineox} \tag{7}$$

The electron-transfer process from dGMP to oxidized intermediates of QDs was also supported by energy level analysis (please see detail in the Supporting Information). Consequently, the quenching is probably resulted from that the reduction of oxidized QDs by dGMP blocks the subsequent annihilation of QD to yield ECL. Third, the influence of resulting oxidation product of dGMP was also assessed. 8-Oxo-dGMP, the well-known major oxidation product of dGMP, was prepared by the H_2O_2-mediated oxidation of dGMP in the presence of ascorbic acid. Amazingly, unlike dGMP, the increasing concentration of 8-oxo-dGMP from 0 to 50 μM significantly quenched the fluorescence of QDs (Supporting Information Figure S5). Identical with fluorescence, the ECL of QDs was also quenched by the addition of 8-oxo-dGMP (Supporting Information Figure S6), but the quenching efficiency of 8-oxo-dGMP (44% quenching at 20 μM 8-oxo-dGMP) was much less than that of dGMP (80% quenching at 5 μM dGMP). This indicates the excited state of QDs could be efficiently quenched by 8-oxo-dGMP. The quenching mechanism is unlikely to be static quenching because no obvious change of adsorption spectra of QDs was observed in the presence of 50 μM 8-oxo-dGMP (Supporting Information Figure S7). Considering the lack of overlap between the emission spectrum of donor QDs and absorption spectrum of acceptor 8-oxo-dGMP, both Förster energy transfer and Dexter energy transfer requiring spectra overlap could be ruled out. We supposed that the electron transfer, rather than energy transfer, was the plausible mechanism for the quenching effect of 8-oxo-dGMP to both QD's FL and ECL. Hence, the dGMP-induced QD's ECL quenching was probably due to the reduction of oxidized QDs and consequential generation of dGMP oxidation product capable of quenching the excited state of QDs. The more efficient quenching of dGMP compared with 8-oxo-dGMP could be explained by that the in situ generation of dGMP oxidation product on the electrode surface increases the localized concentration of quencher.

dx.doi.org/10.1021/ac4004437 | Anal. Chem. XXXX, XXX, XXX−XXX

Different Effects of dGMP and G-Rich DNA on QDs ECL as the Basis of Analytical Applications. It is fascinating to know whether the dGMP residues in the DNA strand are capable of quenching QDs ECL. To address this issue, we have explored the effect to ECL of CdTe/ZnS QDs from different DNA structures, such as ssDNA, double-stranded DNA (dsDNA), and DNA hairpin that contains G base of about the same amount as 2.5 μM dGMP. As shown in Figure 3, except free dGMP residues (Figure 3, curve e), G-rich

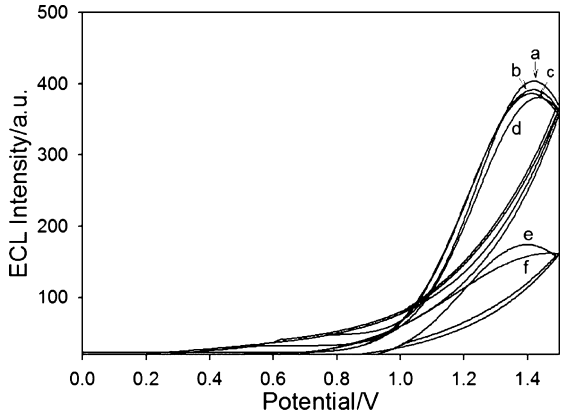

Figure 3. Cyclic ECL curves of 0.05 mg/mL CdTe/ZnS QDs solution before (a) and after addition of 0.25 μM G-rich dsDNA (P1 + P2, b), ssDNA (P2, c), hairpin (SHP-1, d), 2.5 μM dGMP (e), and ssDNA (TAP-2, f) hydrolyzed by Exo I.

ssDNA, dsDNA, and hairpin DNA (Figure 3, curves b–d) all cause negligible ECL quenching, probably resulting from the electrostatic repulsion between the oligonucleotide and negative-charged QDs and steric hindrance of G residue embedded in DNA structures to access QDs. This remarkable difference between dGMP and G-containing DNA in quenching efficiency of QDs ECL is intriguing and presents a promising basis for design of new QDs–ECL-derived analytical applications. To fulfill signal transduction for biosensing, we applied Exo I here to implement the transformation from ssDNA to free dGMP. Exo I degrades ssDNA in a 3′ to 5′ direction and releases deoxyribonucleoside 5′-monophosphates (dNMP) in a stepwise manner. As we can see from Figure 3 (line f), when the G-rich ssDNA was digested by Exo I for 0.5 h, the products could effectively quench the ECL of QDs. It has been discovered that some protein–DNA interactions could stimulate or prohibit the DNA degradation of Exo I.[34,35] Relying on such phenomena, we developed two types of detection modes, signal-on and signal-off, to probe protein–DNA interactions based on the unique dGMP-mediated QDs ECL quenching (Scheme 1). The proof-of-principle results are exhibited as following using SSB and thrombin as models. The ECL quenching curve (Figure 2B) shows a steep slope in the presence of 0–5 μM dGMP, indicating that the most sensitive response of ECL quenching could be obtained in this concentration range of dGMP. In order to achieve sensitive determination of proteins and minimize the detection limit, we choose the DNA concentration in biosensors design that can produce about 2.5 μM dGMP after being completely digested by Exo I. Moreover, the reaction time and the concentration of the Exo I were optimized for further ECL detection. As shown in Supporting Information Figure S8, kinetic studies were performed to inspect the effect of varying concentrations of Exo

Scheme 1. Schematic Presentation of QDs ECL Assays for Protein–DNA Interactions Based on dGMP Quenching[a]

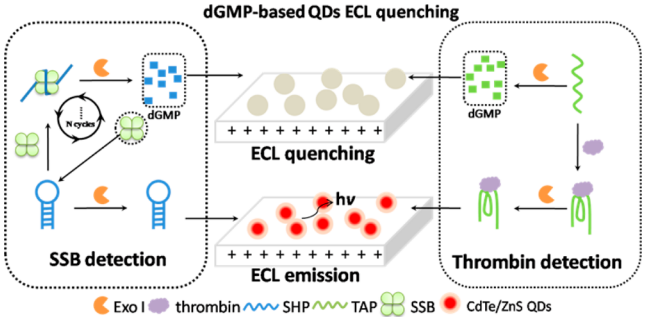

[a]Left part, SSB detection by SSB-simulated cyclic Exo I cleavage; right part, thrombin detection based on the Exo I protection assay.

I on the digestion reactions by monitoring the ECL intensity as a function of time. At low Exo I concentrations (0.2 and 1 U/μL), an obvious retarded stage for ECL quenching in 0–20 min was observed. Considering the balance between the complete cleavage by Exo I and economy of enzyme usage, we chose the moderate concentration of Exo I (2 U/μL) and 30 min reaction time for following experiments.

Signal-Off Detection of SSB by QD ECL Based on SSB-Activated Exo I Cleavage. SSB composed of four identical 18.9 kDa subunits binds with high affinity to single-stranded regions of DNA and plays an essential role as an accessory protein in DNA replication, recombination, and repair. Previous biological research of SSB generally relied on fluorescence techniques, and some linear and hairpin DNA fluorescent probes have been developed.[36,37] However, using ECL methods to study SSB–DNA interaction is still unexplored. Herein, we present a novel QDs ECL biosensor to detect SSB on the basis of SSB-activated Exo I cleavage and unique dGMP-induced QDs ECL quenching, as illustrated in the left part of the Scheme 1. Hairpin DNA probe (SSB hairpin probe, SHP) was exploited here because of its unique loop–stem secondary structure in which the duplex stem can attenuate the ssDNA-specific Exo I cleavage and the loop structure can interact with SSB to trigger hairpin open. Without SSB, SHP retains intact under Exo I treatment, showing no influence on QDs ECL. However, since SSB can stimulate the Exo I activity through its interactions with both ssDNA and Exo I,[34] addition of SSB can induce the switch of SHP to the open state and activate the Exo I to cleavage the resulting linear ssDNA. When the whole DNA strand was digested, released SSB could bind with the other hairpin, and the next enzymatic cycle begins. These binding–cleavage recycles of SHP lead to the release of numerous free dNMP, including dGMP, causing significant QDs ECL quenching in response to SSB.

Three SHPs (SHP-1, SHP-2, and SHP-3, sequences shown in Table 1) with the stem length varied from 5 to 7 were rationally designed to research the different ECL response to SSB. Two design rules were followed; one is a variety of stem length with different stability[38] in order to acquire diverse open efficiency when binding with the SSB; the other is the unified G residue number of 13 in every SHP, guaranteeing the equal quenching capacity for each SHP after its opening. At first, we compared the different efficiencies of SSB-stimulated Exo I cleavage to three SHPs; the results were probed by electrophoresis analysis with a 10% nondenaturing polyacrylamide gel electrophoresis (PAGE) gel (Supporting Information Figure

dx.doi.org/10.1021/ac4004437 | Anal. Chem. XXXX, XXX, XXX–XXX

S9). The identical mobility of SHPs bands before and after Exo I treatment (lanes 1, 4, and 7 compared with lanes 2, 5, and 8) indicates no obvious degradation for all three SHPs in the presence of Exo I only, corresponding with that the secondary structure of SHPs inhibits the exonuclease activity of Exo I. After incubation with SSB and digestion by Exo I, the SHP-1, SHP-2, and SHP-3 were degraded 96.7%, 73.3%, and 60.6%, respectively, which were measured by quantitative comparison of their band darkness after SSB/Exo I treatment (lanes 3, 6, and 9) with their initials (lanes 1, 4, and 7) via Image J. The decreasing degradation efficiency from SHP-1 to SHP-3 was in accordance with their increasing stem stability (stem length from 5 to 7), and SHP-1 was found to be the optimal probe for SSB detection. The sharp single bands near the well of PAGE gel in lanes 3, 6, and 9 were attributed to the complexes of SSB and SHPs. The electrophoresis results are in agreement with our prediction, demonstrating that it is rational to probe SSB by SHPs and provides a solid foundation for the following experiments.

The detection of SSB by our QDs ECL sensor is shown in Figure 4A. When 50 nM SSB was added to the solution of 250 nM SHP-1, the Exo I-catalyzed DNA hydrolysis was activated and then dGMP was released, resulting in that about 88% of the ECL of the CdTe/ZnS QDs was quenched (Figure 4A, line b).

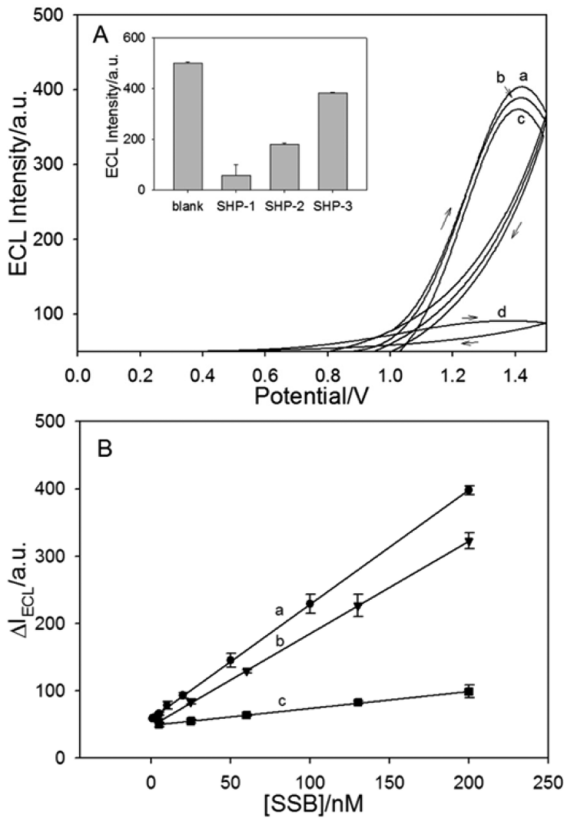

Figure 4. (A) Cyclic ECL curves of CdTe/ZnS QDs before (a) and after addition of 500 nM SSB (b), 250 nM SHP-1 incubated with 2 U/μL Exo I for 0.5 h (c), and 250 nM SHP-1 incubated with 50 nM SSB then digested by 2 U/μL Exo I for 0.5 h (d). The inset shows QDs ECL intensities of QDs measured at +1.38 V responding to 250 nM SHP-1, SHP-2, and SHP-3 incubated with 50 nM SSB, then digested by 2 U/μL Exo I, respectively. (B) Relationship between ECL signal decrease and SSB concentration performed by the proposed sensor with 0.25 μM SHP-1 (a), SHP-2 (b), and SHP-3 (c).

Control experiment showed that SSB only, even at a high concentration (500 nM), could not affect QDs ECL (Figure 4A, line c). The SHP-1 treated by Exo I without SSB also leads to no obvious ECL quenching because of the inhibition of Exo I activity by its hairpin structure (Figure 4A, line d). Next, we used the proposed method to elucidate the effect of hairpin structure on the open efficiency by the SSB; the quenching effects of the SHPs with stem lengths ranging from 5 to 7 bases were compared, as shown in the inset of Figure 4A. It was found that the quenching intensity progressively decreased as the stem length increased, 64% and 23% for the SHP-2 and SHP-3, respectively, which was in accordance with gel results.

The working curves were investigated by adding different concentrations of SSB to the solution of the 0.25 μM of three tested SHPs, respectively. As shown in Figure 4B, different linear increase of the SSB concentration-dependent ECL quenching intensity ($I_0 - I_1$) was observed, resulting from the continuous generation of dGMP catalyzed by Exo I. The sensitivity of SSB detection gradually decreases with the increase of the stem length of SHPs. The calibration curves for detecting the SSB concentrations indicated that the linear range of this dGMP-based SSB assay by SHP-1 is from 1 to 200 nM with a detection limit of 0.1 nM (S/N = 3), and from 5 to 200 nM for the SHP-2 and SHP-3 with a detection limit of 1.2 and 4 nM, respectively. Eleven ECL measurements of the CdTe/ZnS QDs solution upon continuous cyclic scans when assaying 100 nM SSB in pH 9.0 Tris−HCl buffer showed constant signals with relative standard deviation (RSD) of 2.2% (Supporting Information Figure S10). Hence, the present method based on the dGMP quenching of the ECL can be used to detect the concentration of SSB conveniently, reliably, and efficiently.

The selectivity of the sensor for SSB was tested via comparing the ECL signal changes brought by three other proteins: bovine serum albumin (BSA), lysozyme, and thrombin. Supporting Information Figure S11 shows that BSA, lysozyme, and thrombin exhibit no obvious decrease of signal, in contrast to the significant response of sensor to 200 nM SSB. Similarly, a mixed sample (200 nM SSB coexisted with 200 nM BSA, lysozyme, and thrombin) did not exhibit major signal change compared with that of SSB alone. This comparison essentially suggested that the sensor was highly selective and had quite an affinity toward the target protein.

Signal-On Detection of Thrombin Based on Cleavage Protection by Aptameric Binding. Aptamers are structured single-strand nucleic acids capable of specific binding to various molecular targets, which are screened from a SELEX (systematic evolution of ligands by exponential enrichment) process.[39] They have attracted increasing attentions as artificial recognition elements for its high selectivity and binding affinity. The best-known example is one kind of thrombin-binding aptamer, TBA, a single-stranded 15-mer DNA that forms an intramolecular G-quadruplex to interact with thrombin, a protein in the blood coagulation system. On the basis of the aptamer−protein binding complex insusceptible to nuclease hydrolysis,[35] we developed a novel QDs ECL-based aptasensor to signal-on detect thrombin via ECL quenching by dGMP and enzymatic cleavage protection by aptameric binding. Our design strategy is shown in the right part of Scheme 1. Three single-stranded DNA probes, namely, thrombin aptamer probes TAP-1, TAP-2, and TAP-3 (Table 1), were designed, which were composed by the recognition segment at the 3′ end containing the 15-mer thrombin aptamer sequence and G-rich signal-generating

dx.doi.org/10.1021/ac4004437 | Anal. Chem. XXXX, XXX, XXX−XXX

segment at the 5′ end with different lengths as well as G residue numbers. The TAPs would be readily hydrolyzed by Exo I to release dGMP in the absence of thrombin, which then quenches the ECL intensity. When thrombin is added, the aptamer would selectively capture thrombin to form binding complex, which protects bound TAPs against Exo I cleavage and restores QDs ECL. In addition, TAP-1, TAP-2, and TAP-3 contain 9, 13, and 17 G bases, respectively, in total, which is expected to obtain tunable sensitivity of the ECL thrombin sensor because they release different amounts of dGMP after hydrolysis and consequently cause varying degrees of QDs ECL quenching.

Figure 5A shows the typical detection of thrombin by the proposed ECL method. Without thrombin, 76% of QDs ECL

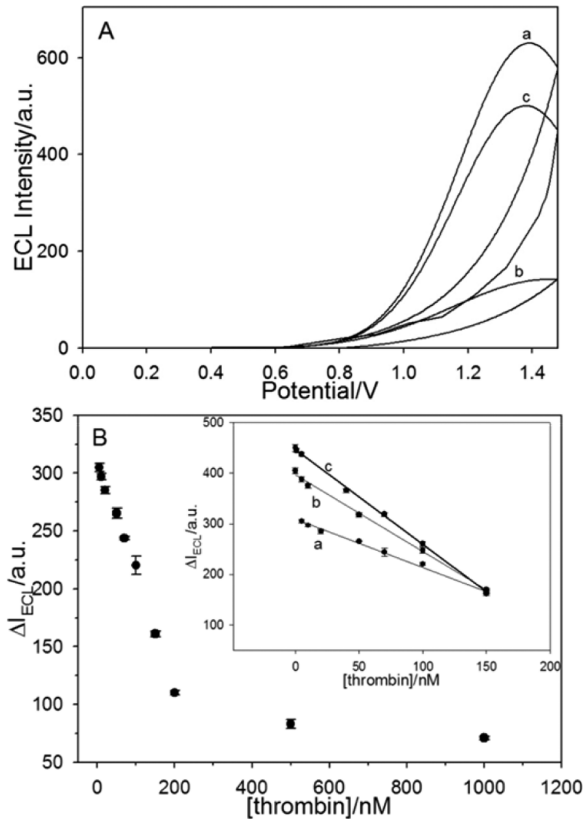

Figure 5. (A) Cyclic ECL curves of 0.05 mg/mL CdTe/ZnS QDs before (a) and after addition of 0.25 μM TAP-2 hydrolyzed by Exo I (b) and 0.25 μM TAP-2 incubated with 0.15 μM thrombin then digested by Exo I (c). (B) Relationship between ECL signal decrease and thrombin concentration performed by the proposed sensor with 0.25 μM TAP-1. The inset shows the liner range for the detection of thrombin with 0.25 μM TAP-1 (a), TAP-2 (b), and TAP-3 (c).

intensity was quenched, indicating the degradation of unbound TAPs by Exo I. However, a weak quenching ECL (19%) of TAP-2 was observed when thrombin binds with the aptamer, which implied that enzymatic digestion was inhibited by aptameric thrombin binding. Thus, the feasibility of the ECL thrombin sensor has been attested. The quantitative detection of the thrombin was conducted by using different concentrations of thrombin incubated with three TAPs (Figure 5B). A plot of ECL quenching of the CdTe/ZnS QDs ($I_0 - I_1$) versus thrombin concentrations revealed a linear response characteristic of ECL sensor using TAP-1 as the probe in the concentration range from 5 to 200 nM, with a detection limit of 1 nM (S/N = 3). Further improvement of the sensitivity was achieved by using TAP-2 and TAP-3 with adding four and eight G bases on the basis of TAP-1, respectively. For TAPs, the more G bases they contain, the more dGMP they could generate after Exo I digestion, the larger signal change thrombin causes. As expected, the calibration curves for thrombin measurement indicates that the linear range of this QD ECL-based assay is from 5 to 150 nM for the TAP-2 with a detection limit of 0.5 nM, and from 1 to 150 nM for the TAP-3 with a detection limit of 0.1 nM. Hence, the present method based on dGMP quenching of QDs is potent for sensitive detection of thrombin and its sensitivity can be facilely regulated by the G base numbers in probe sequence.

In order to examine its selectivity, the thrombin aptasensor was exposed to different nontarget proteins. As shown in Supporting Information Figure S12, only thrombin causes a significant ECL signal while other proteins (BSA and lysozyme) give weak ECL intensity comparable to control in the presence of Exo I. On the other hand, the random sequence in Table 1 was also used to test DNA specificity of thrombin binding; a remarkable ECL quenching was observed demonstrating that the Exo I cleavage protection does not occur due to no thrombin bound to the random sequence. All these control experiments indicate that the aptasensor possesses high selectivity. ECL measurements of the CdTe/ZnS QDs solution upon continuous cyclic scans in air-saturated pH 9.0 Tris−HCl buffer showed constant signals with an RSD of 4.6% (Supporting Information Figure S13), indicating the excellent stability of the proposed sensor. The intra-assay RSDs for three parallel measurements at 5 and 100 nM thrombin with TAP-2 using the same ITO electrode were 3.0% and 4.4%, respectively, indicating a good precision. When the sensor was not in use, it was stored in air condition at room temperature and measured in pH 9.0 HCl−Tris buffer every 2 days. No obvious change in the ECL intensity was observed after storage for 4 weeks.

CONCLUSIONS

In summary, dGMP was observed to quench the anodic ECL of CdTe/ZnS QDs, and a novel QDs ECL biosensing strategy has been developed for detection of protein−DNA interactions based on this unique ECL quenching phenomenon. The plausible quenching mechanism is supposed to the reduction of oxidized CdTe/ZnS QDs by dGMP and the quenching of excited QDs by resulting oxidation product of dGMP. With the Exo I-assisted transformation from ssDNA to dGMP, we implemented the proposed QDs ECL strategy to realize the sensitive and selective detection of SSB and thrombin by two distinct analysis modes: signal-off analysis for SSB by Exo I stimulation and signal-on analysis for thrombin by Exo I protection. This method possesses multifaceted advantages involving label-free merit without QDs or DNA modification, highly tunable sensitivity and dynamic range by facilely changing the G base number in DNA probe, and homogeneous detection avoiding multistep washing and separation. More importantly, due to its modularity and versatility, the proposed ECL QDs method could be immediately extended to a wide variety of DNA-related biosensing, such as nucleic acid analysis relied on enzymatic cleavage amplification,[40] various DNA-binding proteins with different binding modes,[41] and even the small-molecule−protein interaction by terminal protection,[42] which will greatly expand the application of QDs ECL in bioanalysis.

dx.doi.org/10.1021/ac4004437 | Anal. Chem. XXXX, XXX, XXX−XXX

■ ASSOCIATED CONTENT

Supporting Information

Additional information including extensive figures as noted in text. This material is available free of charge via the Internet at http://pubs.acs.org.

■ AUTHOR INFORMATION

Corresponding Author

*Phone: +86-731-88821626. Fax: +86-731-88821848. E-mail: niezhou.hnu@gmail.com.

Notes

The authors declare no competing financial interest.

■ ACKNOWLEDGMENTS

This work was financially supported by the National Basic Research Program of China (973 program nos. 2009CB421601 and 2011CB911002), the Foundation for Innovative Research Groups of NSFC (Grant 21221003), the National Natural Science Foundation of China (nos. 21222507, 21175036, 21190044, and 21075031), the Program for New Century Excellent Talents in University (NCET-10-0366), and the Natural Science Foundation of Hunan Province (no. 10JJ2005). We appreciate Dr. Zhihong Yan, Dr. Yingzhuang Chen, and Huiping Hu for the assistance on HPLC experiments.

■ REFERENCES

(1) Bruchez, M., Jr.; Moronne, M.; Gin, P.; Weiss, S.; Alivisatos, A. P. *Science* **1998**, *281*, 2013−2016.
(2) Chan, W. C. W.; Nie, S. *Science* **1998**, *281*, 2016−2018.
(3) Ma, Q.; Su, X. *Analyst* **2011**, *136*, 4883−4893.
(4) Mansur, H. S. *Wiley Interdiscip. Rev.: Nanomed. Nanobiotechnol.* **2010**, *2*, 113−129.
(5) Shimizu, K.; Woo, W.; Fisher, B.; Eisler, H.; Bawendi, M. *Phys. Rev. Lett.* **2002**, *89*, 117401−117404.
(6) Vaidya, S. V.; Gilchrist, M. L.; Maldarelli, C.; Couzis, A. *Anal. Chem.* **2007**, *79*, 8520−8530.
(7) Medintz, I. L.; Uyeda, H. T.; Goldman, E. R.; Mattoussi, H. *Nat. Mater.* **2005**, *4*, 435−446.
(8) Cheng, L.; Liu, X.; Lei, J.; Ju, H. *Anal. Chem.* **2010**, *82*, 3359−3364.
(9) Wang, J.; Shan, Y.; Zhao, W. W.; Xu, J. J.; Chen, H. Y. *Anal. Chem.* **2011**, *83*, 4004−4011.
(10) Zhou, H.; Liu, J.; Xu, J. J.; Chen, H. Y. *Anal. Chem.* **2011**, *83*, 8320−8328.
(11) Jie, G.; Wang, L.; Yuan, J.; Zhang, S. *Anal. Chem.* **2011**, *83*, 3873−3880.
(12) Jaiswal, J. K.; Simon, S. M. *Trends Cell Biol.* **2004**, *14*, 497−504.
(13) Ding, Z.; Quinn, B. M.; Haram, S. K.; Pell, L. E.; Korgel, B. A.; Bard, A. J. *Science* **2002**, *296*, 1293−1297.
(14) Lei, J.; Ju, H. *Trends Anal. Chem.* **2011**, *30*, 1351−1359.
(15) Zou, G.; Ju, H. *Anal. Chem.* **2004**, *76*, 6871−6876.
(16) Jie, G.; Zhang, J.; Wang, D.; Cheng, C.; Chen, H. Y.; Zhu, J. J. *Anal. Chem.* **2008**, *80*, 4033−4039.
(17) Cui, R.; Gu, Y. P.; Bao, L.; Zhao, J. Y.; Qi, B. P.; Zhang, Z. L.; Xie, Z. X.; Pang, D. W. *Anal. Chem.* **2012**, *84*, 8932−8935.
(18) Wang, J.; Han, H.; Jiang, X.; Huang, L.; Chen, L.; Li, N. *Anal. Chem.* **2012**, *84*, 4893−4899.
(19) Jiang, H.; Ju, H. *Chem. Commun.* **2007**, 404−406.
(20) Liu, X.; Zhang, Y.; Lei, J.; Xue, Y.; Cheng, L.; Ju, H. *Anal. Chem.* **2010**, *82*, 7351−7356.
(21) Jiang, H.; Ju, H. *Anal. Chem.* **2007**, *79*, 6690−6696.
(22) Liu, X.; Jiang, H.; Lei, J.; Ju, H. *Anal. Chem.* **2007**, *79*, 8055−8060.
(23) Wang, Y.; Lu, J.; Tang, L.; Chang, H.; Li, J. *Anal. Chem.* **2009**, *81*, 9710−9715.
(24) Jie, G.; Li, L.; Chen, C.; Xuan, J.; Zhu, J. J. *Biosens. Bioelectron.* **2009**, *24*, 3352−3358.
(25) Jie, G.; Yuan, J. *Anal. Chem.* **2012**, *84*, 2811−2817.
(26) Huang, H.; Jie, G.; Cui, R.; Zhu, J. J. *Electrochem. Commun.* **2009**, *11*, 816−818.
(27) Huang, H.; Tan, Y.; Shi, J.; Liang, G.; Zhu, J. J. *Nanoscale* **2010**, *2*, 606−612.
(28) Bae, Y.; Myung, N.; Bard, A. J. *Nano Lett.* **2004**, *4*, 1153−1161.
(29) Holmberg, R. C.; Tierney, M. T.; Ropp, P. A.; Berg, E. E.; Grinstaff, M. W.; Thorp, H. H. *Inorg.Chem.* **2003**, *42*, 6379−6387.
(30) Armistead, P. M.; Thorp, H. H. *Anal. Chem.* **2001**, *73*, 558−564.
(31) Sistare, M. F.; Holmberg, R. C.; Thorp, H. H. *J. Phys. Chem. B* **1999**, *103*, 10718−10728.
(32) Dennany, L.; Forster, R. J.; Rusling, J. F. *J. Am. Chem. Soc.* **2003**, *125*, 5213−5218.
(33) Johnston, D. H.; Glasgow, K. C.; Thorp, H. H. *J. Am. Chem. Soc.* **1995**, *117*, 8933−8938.
(34) Lu, D.; Myers, A. R.; George, N. P.; Keck, J. L. *Nucleic Acids Res.* **2011**, *39*, 6536−6545.
(35) Wang, X. L.; Li, F.; Su, Y. H.; Sun, X.; Li, X. B.; Schluesener, H. J.; Tang, F.; Xu, S. Q. *Anal. Chem.* **2004**, *76*, 5605−5610.
(36) Li, J. J.; Fang, X.; Schuster, S. M.; Tan, W. *Angew. Chem., Int. Ed.* **2000**, *39*, 1049−1052.
(37) Tan, Y. N.; Lee, K. H.; Su, X. *Anal. Chem.* **2011**, *83*, 4251−4257.
(38) Tsourkas, A.; Behlke, M. A.; Bao, G. *Nucleic Acids Res.* **2002**, *30*, 4208−4215.
(39) Green, L. S.; Jellinek, D.; Jenison, R.; Östman, A.; Heldin, C. H.; Janjic, N. *Biochemistry* **1996**, *35*, 14413−14424.
(40) Zhang, M.; Guan, Y. M.; Ye, B. C. *Chem. Commun.* **2011**, *47*, 3478−3480.
(41) Ou, L. J.; Jin, P. Y.; Chu, X.; Jiang, J. H.; Yu, R. Q. *Anal. Chem.* **2010**, *82*, 6015−6024.
(42) Wu, Z.; Zhen, Z.; Jiang, J. H.; Shen, G. L.; Yu, R. Q. *J. Am. Chem. Soc.* **2009**, *131*, 12325−12332.